CHINESE OPTICS LETTERS

Vol. 21, No. 10 | October 2023

Nonlinearity-induced localization enhancement in Fibonacci-like waveguide arrays [Invited]

Licheng Wang (王立成)[1], Hongfei Bu (步鸿飞)[1], Yang Chen (陈 阳)[2,3,4], Zhennan Tian (田振男)[1*], and Xifeng Ren (任希锋)[2,3,4**]

[1] State Key Laboratory of Integrated Optoelectronics, College of Electronic Science and Engineering, Jilin University, Changchun 130012, China

[2] CAS Key Laboratory of Quantum Information, University of Science and Technology of China, Hefei 230026, China

[3] CAS Synergetic Innovation Center of Quantum Information Quantum Physics, University of Science and Technology of China, Hefei 230026, China

[4] Hefei National Laboratory, University of Science and Technology of China, Hefei 230088, China

*Corresponding author: zhennan_tian@jlu.edu.cn

**Corresponding author: renxf@ustc.edu.cn

Received March 29, 2023 | Accepted May 5, 2023 | Posted Online August 23, 2023

Based on the one-dimensional periodic and Fibonacci-like waveguide arrays, we experimentally investigate localized quantum walks (QWs), both in the linear and nonlinear regimes. Unlike the ballistic transport behavior in conventional random QWs, localization of QWs is obtained in the Fibonacci-like waveguide arrays both theoretically and experimentally. Moreover, we verify the enhancement of the localization through nonlinearity-induced effect. Our work provides a valid way to study localization enhancement in QWs, which might broaden the understanding of nonlinearity-induced behaviors in quasi-periodic systems.

Keywords: Fibonacci-like waveguide arrays; nonlinearity-induced effect; localization enhancement.
DOI: 10.3788/COL202321.101301

1. Introduction

Over the past decades, quantum walks (QWs) have evolved into an essential model applied in the field of quantum computing[1], quantum algorithms[2], and quantum simulations[3], where monumental progress has been made. Hitherto, discrete-time and continuous-time QWs have been studied both theoretically and experimentally in various systems, including cold atoms[4], electrons[5], trapped ions[6], and photons[7,8]. Notably, photonic systems, in particular integrated optical waveguides, construct a multifunctional and easily accessible platform for performing discrete-time or continuous-time QWs, with the help of cascade beam splitters[9] or waveguide arrays[10]. One of the exclusive phenomena in QWs is the localization caused by the existence of disorder, known as Anderson localization[11]. By disrupting the periodicity of the system in time or space, the dynamics of the system can be determined, and the localization effect can be maintained. Due to the advantage of robust information transfer, such effects have been utilized to protect the transmission of quantum states in quantum photonic systems[12–17].

The quasi-periodic systems, which are neither periodic nor disordered, exhibit critical nature and localized QWs (LQWs)[13,15,17]. Distribution of the lattice potential or tunneling of such systems are modulated quasi-periodically, but lack translational symmetry. One of the models is based on the Fibonacci sequence, whose modulation strength is of the golden ratio 1.618[18]. LQWs have been theoretically proposed in Fibonacci-like waveguide arrays (FWAs) with diagonal and off-diagonal quasi-periodic modulations, and in Ref. [15,19], both the lattice potential and tunneling were tuned. However, as proposed in previous works, QWs on Fibonacci tight-binding models are actually not localized. The eigenstates are critical and wave packet dynamics is known to be diffusive[12,20]. Although a multicore fiber platform has been introduced to experimentally demonstrate the LQWs, which proves LQWs could be observed due to the short propagation, the sample preparation process is a little bit complicated[19]. Also, study on the LQW effect, particularly the influence of nonlinear-induced interaction[21], still remains to be further verified. Thanks to the development of precise processing technique, an ultrafast laser micromachining method has been proposed. It has the capability of generating refractive index change and leaving three-dimensional tracks inside transparent materials and hence yields a favorable tool for direct writing optical waveguides[22–28]. Via fast prototyping and controlling the spacing between evanescently coupled waveguides, FWAs with both diagonal and off-diagonal modulations can be realized. The waveguide transmission length represents the evolution time, while the distribution of energy of the

waveguide end face at certain length reflects the real-time evolutionary dynamics[10].

In this Letter, we experimentally investigate LQWs in FWAs with both diagonal and off-diagonal modulations. By monitoring the light propagation dynamics in periodic waveguide arrays (PWAs) and FWAs, we find that the localization of QWs can be obtained in FWAs compared to the discrete diffraction patterns observed in conventional random QWs. Moreover, as we increase the input peak power, we verify that the localization can be further enhanced in our FWAs when the nonlinearity of light is taken into account.

2. Model and Method

The proposed FWAs consist of two types of waveguides with different propagation constants and the same separation distances, as shown in Fig. 1(a). Our quasi-periodic system is described by a tight-binding Hamiltonian that satisfies the following discrete nonlinear Schrödinger equation[29]:

$$i\frac{\partial \psi_n}{\partial z} + \beta_n \psi_n + C_{n,n-1}\psi_{n-1} + C_{n,n+1}\psi_{n+1} + \gamma|\psi_n|^2\psi_n = 0, \tag{1}$$

where n is the site index, ψ is the hopping amplitude, z is the space coordinate, β is the propagation constant, and γ is the nonlinear coefficient. Note that γ indicates the strength of nonlinearity modulation, and the system remains in the linear regime when $\gamma = 0$.

In our experiment, we use the femtosecond laser-inscribing technique to fabricate the proposed PWAs and FWAs [shown in Fig. 1(b)], at a laser pulse duration of 239 fs, repetition rate of 1 MHz, and working wavelength of 1030 nm. A liquid crystal-based spatial light modulator (LC-SLM, HAMAMATSU X13138-type) is introduced to our experiment to manipulate both the shape and the size of the beam focal spot so as to increase the circularity of the cross section of the waveguides[30,31]. Laser pulses are focused into the borosilicate glass substrate through a 50× objective lens (NA 0.75) assisted with high-precision three-axis air-bearing linear motion stage (Aerotech Inc.) motorizing the substrate. Our FWA is composed of all elements of the Fibonacci series from the first order to the sixth order arranged in sequence, where the total number of the waveguides is 39, as presented in Fig. 1(c), while compared to the FWA, the PWA consists of 39 identical waveguides instead. In order to achieve waveguides with different effective refractive indices, the substrate is motorized at constant velocities of 10 and 40 mm/s. The relationship between mode field diameters and the scanning speeds is shown in Fig. 2(a).

In order to characterize the change of the effective refractive indices for the waveguides fabricated at different scanning speeds, we introduce a directional coupler (DC) consisting of two evanescently coupled waveguides. Note that when injecting light into one arm of the DC, the power splitting ratio α can be defined as stated below, based on a coupled mode equation[32],

$$\alpha = \frac{P_2}{P_1 + P_2} = \sigma^2 \cdot \sin^2\left(\frac{\kappa}{\sigma}\cdot d + \phi\right), \tag{2}$$

and it is important to know the values of coupling coefficient κ and coupling length d, which influence the splitting ratio. For a DC with a coupling length d, the splitting ratio changes when applying a dephasing term σ to alter the amplitude,

$$\sigma = 1/\sqrt{1 + \left(\frac{\Delta\beta}{2\kappa}\right)^2}. \tag{3}$$

Finally, the refractive index change Δn for the two arms of the DC can be determined by

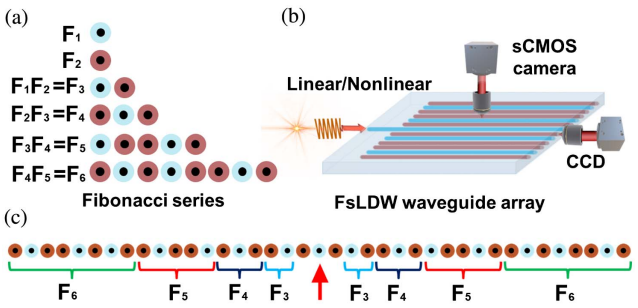

Fig. 1. (a) Scheme of FWAs. Light blue and dark red denote waveguides with different n. F_1 to F_6 indicate the first to sixth orders of the Fibonacci sequences. (b) Schematic of the experimental setup used for verifying QWs in different waveguide arrays; both of the propagation dynamics and end-face energy distributions can be acquired by corresponding high-resolution microscopic observation systems with an sCMOS camera and CCD, respectively. Note that the centermost waveguide is extended from the whole array for easy injecting light. (c) Geometrically symmetrical FWAs designed with all basic elements from F_1 to F_6. The red arrow denotes the specific waveguide for injecting light.

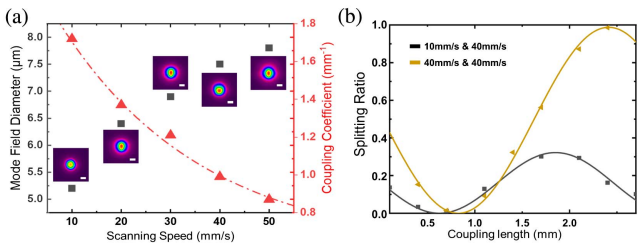

Fig. 2. (a) Relationship between mode field diameters (black cubes), coupling coefficients between two evanescently coupled waveguides, where one is scanned at 40 mm/s and the other at 10 to 50 mm/s, respectively (red triangles), and the scanning speeds. Mode field distributions of certain scanning speeds are shown. The scale bar is 2 μm. (b) Relationship between splitting ratio and coupling length for a symmetry DC (both arms are scanned at 40 mm/s) and an asymmetry DC (one arm is scanned at 10 mm/s, and the other is scanned at 40 mm/s); black cubes and yellow triangles denote experimental data at the scanning speeds of 10 and 40 mm/s, respectively, and the corresponding sinusoidal lines are fitted results.

$$\Delta n = \frac{\lambda_o \Delta\beta}{2\pi}. \tag{4}$$

For a symmetry DC with two identical waveguides fabricated at a scanning speed of 40 mm/s, the maximum power coupling ratio σ^2 is approximately 1. The yellow triangles stand for coupling ratios acquired from a series of DCs with various coupling lengths ranging from 0 to 3 mm [shown in Fig. 2(b)]. When one of the waveguides of a DC is fabricated at the scanning speed of 10 mm/s, the maximum power coupling ratio is altered by the asymmetry, and the related refractive index change Δn can be used to tune the splitting ratio. According to the relationship between the power-splitting ratio and the coupling length, we can learn that σ^2 is 0.9875 for waveguides fabricated at 40 mm/s, while it is 0.3221 for those fabricated at 10 mm/s. Note that as the scanning speed increases, the related coupling coefficient for the waveguides follows an exponential decay [fitted red dashed line shown in Fig. 2(a)]. The coupling coefficients are 0.9901 and 1.7210 for waveguides fabricated at 40 and 10 mm/s, respectively. Then we come to the conclusion that the difference between the effective refractive index for the scanning speed at 10 and 40 mm/s in our experiment is approximately 0.0005, which is also used for further numerical simulations.

3. Results and Discussion

We study QWs in quasi-periodic waveguide arrays with Fibonacci-like modulation by injecting light into a single site. Using a beam propagation method (BPM)[33], with simple parameters like an effective refractive index, coupling distance, and coupling strength between the neighboring evanescent coupling waveguides, we can numerically predict the behaviors of the light propagation dynamics not only in the PWAs, but also in our quasi-periodic FWAs, even when nonlinear perturbation is taken into account. It is necessary to emphasis that single-photon QWs exhibit similar behaviors compared to classical wave dynamics due to the fact that evolution of the coherent states can be viewed as multiple independent single-photon QWs; thus the energy distributions follow the same rule as the detecting probabilities of photon distribution at certain output end faces[33].

We show numerical calculation results of QWs in our designed PWA and FWA. In the PWA, the total number of waveguides is set to be 39, which ensures the size of the PWA is the same as that of the FWA. The single-site excitation is applied to the centermost waveguides of the PWA and FWA. As shown in Fig. 1(c), an FWA will transform into a PWA when the basic composition waveguide F_1 and F_2 are identical. The waveguide separation distance between near-neighboring waveguides is fixed at 8 μm, and the effective refractive index difference between F_1 and F_2 is set as 0.0005 in the FWA, as stated earlier. In a PWA, random QWs could be observed, and the light slowly diffuses as it propagates. Compared to the discrete diffraction pattern shown in Fig. 3(a1), the light propagation dynamics in the FWA is different. As the propagation distance increases, the transmission of light in the FWA is "localized" in the range of a few waveguides at the center [shown in Fig. 3(b1)].

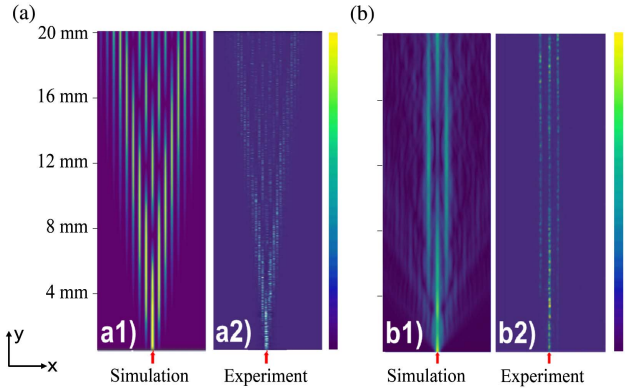

Fig. 3. Propagation dynamics of single excitation. (a1) Theoretical and (a2) experimental results for periodic waveguide arrays, where F_1 and F_2 are identical. (b1) Theoretical and (b2) experimental results for FWAs, where F_1 and F_2 are different. The total length of the propagation is 20 mm, and the coordinate y denotes the propagation direction.

To provide a thorough view of the propagation dynamics, we inject light at a wavelength of 800 nm into the single lattice site from the centermost waveguide. The evolution of the wave dynamics is revealed by observing the scattered light at the top of the sample [shown in Fig. 1(b)]. The strength of the scattered signal is locally proportional to the intensity of the propagating light at a specific position[33]. As a result, we can obtain the entire photon evolution dynamics of the system by observing the scattered signal of the chain instead of intercepting different lengths. Considering that our working wavelength is near-infrared, we use a coaxial imaging system with an Andor Zyla 5.5 sCMOS camera, which has a high resolution of 5.5 megapixels and ideal ultralow noise performance, to fully characterize and better analyze the weak surface scattered signal. Due to the limited field of view of the observing system, we cannot obtain the whole evolution dynamics at one certain position. Hence, we choose to take a series of pictures at different propagation lengths along the propagation direction and finally stitch them together. Finally, the recovered evolution dynamics can be obtained and fully presented in Figs. 3(a) and 3(b).

In a PWA, the effective refractive index of F_1 and F_2 remains the same, and random QWs could be experimentally observed, where the light slowly symmetrically diffuses to the whole arrays as they propagate [shown in Fig. 3(a2)] and exhibits good agreement with the numerical simulations presented in Fig. 3(a1). As for QWs in the FWAs, with the help of direct imaging of the entire light propagation process, the localization of light is clearly presented, and the experimental result [shown in Fig. 3(b2)] satisfies the previous prediction we made. We obtain intensity distribution not only from the surface scattered light of the waveguide arrays, but also from the end-face output. The intensity distribution of the end-face output is obtained using an objective lens and a CCD to directly monitor the end face

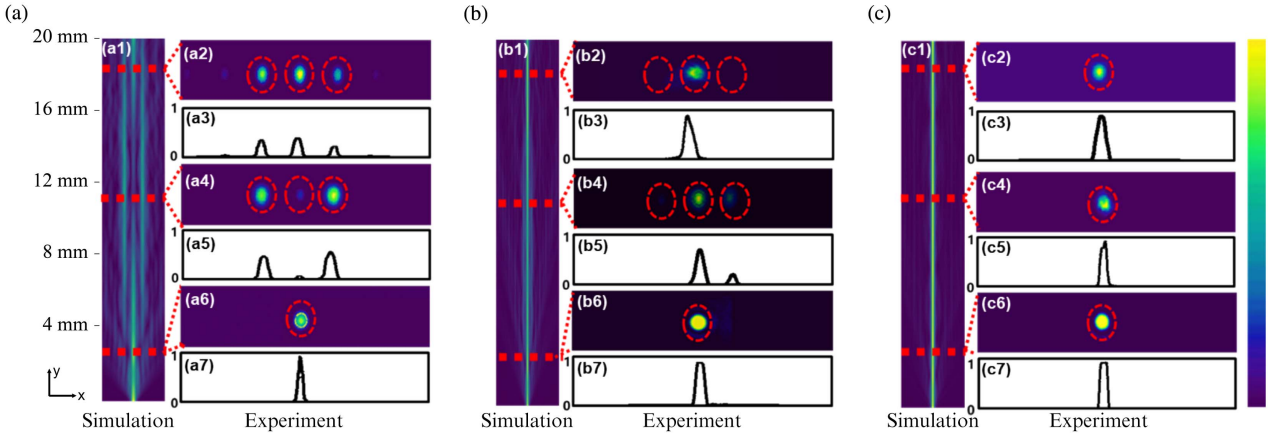

Fig. 4. Propagation dynamics in the waveguide arrays without/with nonlinear perturbation excitation. (a1), (b1), and (c1) show simulated results for injecting linear ($\gamma = 0$), nonlinear ($\gamma = 0.2$), and strongly nonlinear ($\gamma = 0.5$) lights, respectively. (a2), (a4), and (a6); (b2), (b4), and (b6); and (c2), (c4), and (c6) are experimental results of the end-face energy distributions for the waveguide arrays at different coupling lengths (3, 11, and 18 mm), while (a3), (a5), and (a7); (b3), (b5), and (b7); and (c3), (c5), and (c7) are the extracted normalized strengths for the energy distributions. The nonlinear coefficient γ is in the unit of m^{-1} W^{-1}, and we choose the dimensionless quantities for simulations. The coordinate y denotes the propagation direction.

of different samples with coupling lengths of 3, 11, and 18 mm, respectively [shown in Fig. 4]. Our experimental results indicate that the end-face output behaves similar to the surfaced scattered light energy distribution and prove that localization of light could be observed in FWAs at a short propagation distance[12].

The effect of nonlinearity on localized states in our FWAs is studied by a single-site excitation. We excite our FWAs to exhibit self-focusing by carefully controlling the injected energy into the centermost waveguide, which ensures that the experiments are done in the weak nonlinear regime. According to our numerical simulations, nonlinear perturbation will significantly affect the propagation constant of the waveguide due to the Kerr nonlinear effect[21,34], and therefore leads to enhanced localization in our FWAs, where the related nonlinear coefficient γ is set to be 0.2 and 0.5, respectively [shown in Figs. 4(b1) and 4(b2)]. Note that the larger the perturbation is, the stronger the localization will be. Our experimental results prove once again that the localized mode exhibits a significant response to nonlinearity. When the input peak power reaches 1.2 MW, enhanced localization of QWs could be observed, as is shown in Figs. 4(b2) to 4(b7). After increasing the input peak power to 1.9 MW, the localization becomes stronger, and only in the centermost waveguide will the output energy be observed at all measured coupling lengths [shown in Figs. 4(c2) to 4(c7)]. These results can be explained according to the theory raised in Ref. [34]. When the refractive index increases due to the nonlinear effect but the physical sizes of the cores are not changed, the mode field diameter is reduced. As a result, light is strongly confined in the cores. Coupling this effect with deterministic disorder by a quasi-periodic structure, enhancement of LQW can be realized, as shown in Figs. 4(b) and 4(c). In fact, when light walks among PWAs, such nonlinearity also leads to the localization effect, and the threshold of nonlinear effect in FWAs is lower due to a larger mismatch of propagation constant and coupling coefficient.

4. Conclusion

In summary, we have studied LQWs in one-dimensional FWAs with both diagonal and off-diagonal quasi-periodic modulations. We implement an effective change in the waveguide refractive index by controlling the laser scanning speed, thus modulating the propagation constant and coupling coefficient. Through direct imaging, we monitor the entire process of QWs in the waveguide arrays with a single-site excitation and validate LQWs in the FWAs. Furthermore, we experimentally demonstrate enhanced LQWs when weak nonlinear light is induced. As previously stated, although we mainly focus on Fibonacci-like modulations in this work, the proposed ideas can be generally available for studying LQWs in other quasi-periodic structures[20]. Our work may contribute a new foundation to the study of localization enhancement in QWs and sufficiently broaden the understanding of nonlinear-induced behaviors in quasi-periodic systems[35,36].

Acknowledgement

This research was supported by the National Natural Science Foundation of China (Nos. 61825502, 62061160487, and 12204462), the China Postdoctoral Science Foundation (Nos. 2022M723061 and 2019M651200), the Major Science and Technology Projects in Jilin Province (No. 20220301002GX), and the Fundamental Research Funds for the Central Universities. This work was partially carried out at the USTC Center for Micro and Nanoscale Research and Fabrication.

References

1. X. G. Qiang, T. Loke, A. Montanaro, K. Aungskunsiri, X. Q. Zhou, J. L. O'Brien, J. B. B. Wang, and J. C. F. Matthews, "Efficient quantum walk on a quantum processor," Nat. Commun. **7**, 11511 (2016).
2. J. P. Keating, N. Linden, J. C. F. Matthews, and A. Winter, "Localization and its consequences for quantum walk algorithms and quantum communication," Phys. Rev. A **76**, 012315 (2007).
3. J. B. Spring, B. J. Metcalf, P. C. Humphreys, W. S. Kolthammer, X. M. Jin, M. Barbieri, A. Datta, N. Thomas-Peter, N. K. Langford, D. Kundys, J. C. Gates, B. J. Smith, P. G. R. Smith, and I. A. Walmsley, "Boson sampling on a photonic chip," Science **339**, 798 (2013).
4. Y. Lahini, M. Verbin, S. D. Huber, Y. Bromberg, R. Pugatch, and Y. Silberberg, "Quantum walk of two interacting bosons," Phys. Rev. A **86**, 011603 (2012).
5. F. Carbone, "An electron walks into a quantum bar," Science **373**, 1309 (2021).
6. H. Schmitz, R. Matjeschk, C. Schneider, J. Glueckert, M. Enderlein, T. Huber, and T. Schaetz, "Quantum walk of a trapped ion in phase space," Phys. Rev. Lett. **103**, 090504 (2009).
7. T. Giordani, E. Polino, S. Emiliani, A. Suprano, L. Innocenti, H. Majury, L. Marrucci, M. Paternostro, A. Ferraro, N. Spagnolo, and F. Sciarrino, "Experimental engineering of arbitrary qudit states with discrete-time quantum walks," Phys. Rev. Lett. **122**, 020503 (2019).
8. Y. Wang, B. Y. Xie, Y. H. Lu, Y. J. Chang, H. F. Wang, J. Gao, Z. Q. Jiao, Z. Feng, X. Y. Xu, F. Mei, S. T. Jia, M. H. Lu, and X. M. Jin, "Quantum superposition demonstrated higher-order topological bound states in the continuum," Light Sci. Appl. **10**, 8 (2021).
9. A. Crespi, R. Osellame, R. Ramponi, V. Giovannetti, R. Fazio, L. Sansoni, F. De Nicola, F. Sciarrino, and P. Mataloni, "Anderson localization of entangled photons in an integrated quantum walk," Nat. Photonics **7**, 322 (2013).
10. H. Tang, C. Di Franco, Z. Y. Shi, T. S. He, Z. Feng, J. Gao, K. Sun, Z. M. Li, Z. Q. Jiao, T. Y. Wang, M. S. Kim, and X. M. Jin, "Experimental quantum fast hitting on hexagonal graphs," Nat. Photonics **12**, 754 (2018).
11. P. W. Anderson, "Absence of diffusion in certain random lattices," Phys. Rev. **109**, 1492 (1958).
12. Y. Lahini, R. Pugatch, F. Pozzi, M. Sorel, R. Morandotti, N. Davidson, and Y. Silberberg, "Observation of a localization transition in quasiperiodic photonic lattices," Phys. Rev. Lett. **103**, 013901 (2009).
13. J. Ghosh, "Simulating Anderson localization via a quantum walk on a one-dimensional lattice of superconducting qubits," Phys. Rev. A **89**, 022309 (2014).
14. M. Verbin, O. Zilberberg, Y. Lahini, Y. E. Kraus, and Y. Silberberg, "Topological pumping over a photonic Fibonacci quasicrystal," Phys. Rev. B **91**, 064201 (2015).
15. D. T. Nguyen, D. A. Nolan, and N. F. Borrelli, "Localized quantum walks in quasi-periodic Fibonacci arrays of waveguides," Opt. Express **27**, 886 (2019).
16. Y. Chen, X.-M. Chen, X.-F. Ren, M. Gong, and G.-C. Guo, "Tight-binding model in optical waveguides: design principle and transferability for simulation of complex photonics networks," Phys. Rev. A **104**, 023501 (2021).
17. T. Kiss and I. Jex, "Photons walk on fractal graphs," Nat. Photonics **15**, 641 (2021).
18. P. Ribeiro, P. Milman, and R. Mosseri, "Aperiodic quantum random walks," Phys. Rev. Lett. **93**, 190503 (2004).
19. D. T. Nguyen, T. A. Nguyen, R. Khrapko, D. A. Nolan, and N. F. Borrelli, "Quantum walks in periodic and quasiperiodic Fibonacci fibers," Sci. Rep. **10**, 10 (2020).
20. M. A. Pires and S. M. D. Queiros, "Quantum walks with sequential aperiodic jumps," Phys. Rev. E **102**, 15 (2020).
21. L. J. Maczewsky, M. Heinrich, M. Kremer, S. K. Ivanov, M. Ehrhardt, F. Martinez, Y. V. Kartashov, V. V. Konotop, L. Torner, D. Bauer, and A. Szameit, "Nonlinearity-induced photonic topological insulator," Science **370**, 701 (2020).
22. Z. Z. Li, L. Wang, H. Fan, Y. H. Yu, H. B. Sun, S. Juodkazis, and Q. D. Chen, "O-FIB: far-field-induced near-field breakdown for direct nanowriting in an atmospheric environment," Light Sci. Appl. **9**, 7 (2020).
23. X. Q. Liu, Y. L. Zhang, Q. K. Li, J. X. Zheng, Y. M. Lu, S. Juodkazis, Q. D. Chen, and H. B. Sun, "Biomimetic sapphire windows enabled by inside-out femtosecond laser deep-scribing," Photonix **3**, 13 (2022).
24. J. Lapointe, J.-P. Berube, Y. Ledemi, A. Dupont, V. Fortin, Y. Messaddeq, and R. Vallee, "Nonlinear increase, invisibility, and sign inversion of a localized fs-laser-induced refractive index change in crystals and glasses," Light Sci. Appl. **9**, 64 (2020).
25. F. Yu, X.-L. Zhang, Z.-N. Tian, Q.-D. Chen, and H.-B. Sun, "General rules governing the dynamical encircling of an arbitrary number of exceptional points," Phys. Rev. Lett. **127**, 253901 (2021).
26. Y. Zhao, Y. Chen, Z.-S. Hou, B. Han, H. Fan, L.-H. Lin, X.-F. Ren, and H.-B. Sun, "Polarization-dependent Bloch oscillations in optical waveguides," Opt. Lett. **47**, 617 (2022).
27. X.-L. Zhang, F. Yu, Z.-G. Chen, Z.-N. Tian, Q.-D. Chen, H.-B. Sun, and G. Ma, "Non-Abelian braiding on photonic chips," Nat. Photonics **16**, 390 (2022).
28. Y.-K. Sun, X.-L. Zhang, F. Yu, Z.-N. Tian, Q.-D. Chen, and H.-B. Sun, "Non-Abelian Thouless pumping in photonic waveguides," Nat. Phys. **18**, 1080 (2022).
29. D. N. Christodoulides, F. Lederer, and Y. Silberberg, "Discretizing light behaviour in linear and nonlinear waveguide lattices," Nature **424**, 817 (2003).
30. P. S. Salter and M. J. Booth, "Adaptive optics in laser processing," Light Sci. Appl. **8**, 16 (2019).
31. Z.-Z. Li, X.-Y. Li, F. Yu, Q.-D. Chen, Z.-N. Tian, and H.-B. Sun, "Circular cross section waveguides processed by multi-foci-shaped femtosecond pulses," Opt. Lett. **46**, 520 (2021).
32. T. Will, J. Guan, P. S. Salter, and M. J. Booth, "Trimming laser-written waveguides through overwriting," Opt. Express **28**, 28006 (2020).
33. L. C. Wang, Y. Chen, M. Gong, F. Yu, Q. D. Chen, Z. N. Tian, X. F. Ren, and H. B. Sun, "Edge state, localization length, and critical exponent from survival probability in topological waveguides," Phys. Rev. Lett. **129**, 173601 (2022).
34. Y. Lahini, A. Avidan, F. Pozzi, M. Sorel, R. Morandotti, D. N. Christodoulides, and Y. Silberberg, "Anderson localization and nonlinearity in one-dimensional disordered photonic lattices," Phys. Rev. Lett. **100**, 013906 (2008).
35. C. M. Huang, C. Shang, J. Li, L. W. Dong, and F. W. Ye, "Localization and Anderson delocalization of light in fractional dimensions with a quasi-periodic lattice," Opt. Express **27**, 6259 (2019).
36. S. Longhi, "Topological Anderson phase in quasi-periodic waveguide lattices," Opt. Lett. **45**, 4036 (2020).